MIMO Capacity in Hallways and Adjacent Rooms

Dana Porrat*, Persefoni Kyritsi† and Donald C. Cox*
*Electrical Engineering Department, Stanford University, Stanford, CA, USA
†Center for PersonKommunikations, Aalborg University, Aalborg, Denmark
dporrat@wireless.stanford.edu, persa@cpk.auc.dk, dcox@spark.stnaford.edu

Abstract—**Channel capacity in a waveguide with mode coupling is limited by a keyhole effect caused by the propagation mechanism. The coupling among the propagating modes reduces the channel rank, and at sufficient distances between the transmitter and receiver, the channel rank converges to 1. Measurements of the received power and channel capacity along a hallway and in rooms beside it, show a decrease of capacity with distance, which explained by the keyhole effect in the hallway.**

I. Introduction

Multiple antenna systems received a lot of attention in recent years, because of the promise they hold for very large capacities. High capacities are available when the sub-channels connecting each transmit antenna to each receive antenna are independent. Any coupling among these sub-channels causes reduced capacity. Two types of interaction among the sub-channels are:

- Correlation among the sub-channels, which may result from scattering off objects near the transmitter or the receiver.
- Keyhole propagation [1], [2], which is caused by similarity of the propagation paths.

Both types of interaction reduce the rank of the channel matrix. In this paper we investigate the limits on capacity, set by the propagation of radio waves in an indoor hallway that is modeled as a waveguide. The channel is decomposed into the waveguide modes and the coupling among them reduces the channel matrix rank. The mechanism we discuss may cause high antenna correlation and a keyhole effect, depending on the extent of local scattering near the transmitter and receiver. High antenna correlation is expected for systems with little scattering near the transmitter and receiver; A significant keyhole effect is present for systems with a lot of local scattering at both ends. This is the situation in our measurements.

II. Theoretical Analysis

A. Channel Capacity

The general framework we consider is a linear time invariant narrowband channel model:

$$\underline{y} = T\underline{x} + \underline{n} \quad (1)$$

where $\underline{y}$ is the received signal vector with N_r entries, $\underline{x}$ is the $N_t \times 1$ transmit vector and $\underline{n}$ is the $N_r \times 1$ noise vector. The noise at different antennas is assumed independently white Gaussian with average power σ^2. T is the $N_r \times N_t$ complex channel matrix, and we define the normalized channel matrix $H = \frac{1}{g}T$, where $g^2 = \frac{1}{N_t N_r}\sum_i \sum_j |T_{ij}|^2$.

The channel capacity for the case that each transmit antenna transmits with average power P_a is given by [3]:

$$C = \log_2(\det(I + \frac{P_a}{\sigma^2} TT^H)) = \log_2(\det(I + \frac{\rho}{N_t} HH^H)) \quad (2)$$

where ρ is the average SNR at each receiver branch and $()^H$ signifies the conjugate transpose operation.

B. The Channel Model - Ideal Waveguide

We proceed to express the channel matrix T for an indoor hallway environment, following the notation of [4]. Consider a rectangular hollow waveguide, where the x (horizontal) dimension is $2a$ and the y (vertical) dimension is $2b$. The z axis runs along the waveguide and the x and y axes are aligned with the sides of the waveguide. The waveguide modes act as eigen–functions of the structure, in the sense that power can only propagate in a modal fashion. The modes are of either of two polarization: transverse electric (TE) with zero electric field in the z direction, and transverse magnetic (TM), with zero magnetic field in the z direction. The variation of the electric field across the waveguide is described in table I. These expression hold strictly for perfectly conducting waveguides and approximately for lossy dielectric waveguides. The wave vector of the $(p,q)^{\text{th}}$ mode is composed of the components $(\frac{u_{x,p}}{a}, \frac{u_{y,q}}{b}, \beta_{p,q})$ and the change of phase along the z axis is $e^{-j\beta_{p,q}z}$. The components of the wave vector are determined from the boundary conditions at the walls of the waveguide. In practical waveguides, the number of modes for each polarization is approximately $16ab/\lambda^2$. We shall consider modes of both polarizations (TE and TM),

TABLE I
Modes in a rectangular waveguide

	TE	TM
E_x	$\cos\left(\frac{u_{x,p}}{a}x\right)\sin\left(\frac{u_{y,q}}{b}y\right)$	$\cos\left(\frac{u_{x,p}}{a}x\right)\sin\left(\frac{u_{y,q}}{b}y\right)$
E_y	$\sin\left(\frac{u_{x,p}}{a}x\right)\cos\left(\frac{u_{y,q}}{b}y\right)$	$\sin\left(\frac{u_{x,p}}{a}x\right)\cos\left(\frac{u_{y,q}}{b}y\right)$

0-7803-7632-3/02/$17.00 ©2002 IEEE

use L for the total number of propagating modes, and index the modes with a single index n instead of the double index used so far.

Consider a set of transmitting antennas in a waveguide situated at $z = 0$. The i^{th} antenna excites the waveguide modes with amplitudes $\underline{A}_i(0) = [A_{1,i}, A_{2,i}, \ldots A_{L,i}]^T$ when it transmits a unit signal. We form the matrix A by stacking the vectors $\underline{A}_i$ next to each other. It contains the complex amplitudes of all the modes, excited by all the antennas, so the (n, i) entry contains the excitation of the n^{th} mode by the i^{th} antenna. A lossless waveguide with smooth walls does not induce variations in the modal amplitudes so in this case the modal amplitudes are fixed at $A(z) = A(0)$.

The electric field received by the j^{th} receiving antenna, located at (x, y, z), is expressed as a sum of modes. The x component of the field is

$$E_x = \sum_{n=1}^{L} A_n \cos(\frac{u_{x,n}}{a}x) \sin(\frac{u_{y,n}}{b}y) e^{-j\beta_n z} \qquad (3)$$

with a similar expression for the y component of the field. In the absence of noise, the received field in all the receiver antennas $\underline{E}_r$ is expressed in a matrix equation:

$$\underline{E}_r = VZA\underline{E}_t \qquad (4)$$

where $\underline{E}_t$ is a $N_t \times 1$ vector containing the transmitted signals at the N_t transmit antennas. The matrix Z is an $L \times L$ diagonal matrix with the elements $e^{-j\beta_n z}$ on the diagonal. The matrix V is an $N_r \times L$ matrix that contains the contribution of each mode to the signal received on each receiver antenna. Its (i, n) element is

$$\left\{ \begin{array}{c} \cos \\ \sin \end{array} \right\} (\frac{u_{x,n}}{a}x_i) \left\{ \begin{array}{c} \sin \\ \cos \end{array} \right\} (\frac{u_{y,n}}{b}y_i) \qquad (5)$$

where (x_i, y_i) are the components of the location of the i^{th} receiver antenna and cos or sin are chosen according the the antenna polarization. The matrix A is the excitation matrix determined by the transmitter location. We assume that all the receiver antennas are located at the same z coordinate.

By comparing (1) and (4) we see that the channel transfer matrix is given by

$$T = PA \qquad (6)$$

where $P = VZ$ contains the geometry of the receiver and A describes the excitation.

C. *The Channel Model - Waveguide with Loss and Coupling*

In an ideal waveguide (with no loss and no mode coupling) the modal amplitudes are fixed at the transmitter location $z = 0$. In a real waveguide there is loss and coupling among the modes, and we consider a linear coupling model which is described by an equation of the form:

$$\frac{\partial A}{\partial z} = \Gamma A \qquad (7)$$

The diagonal elements $\Gamma_{n,n}$ contain the loss coefficients of each mode. The off-diagonal element $\Gamma_{n,m}$ contains the coupling factor from mode m to mode n. The average coupling factors between any pair of modes depend on the electrical properties of the waveguide walls, the waveguide dimensions and the statistics of the wall perturbations. The coupling matrix for a slab waveguide is given in [5].

The linear coupling model is a first order approximation. It relies on the assumption of slow coupling among the propagating modes [6], that is justified in the case of small perturbations in the geometry of the waveguide.

We use the waveguide mode analysis with the linear coupling model to study the effect of coupling on the capacity of radio channels propagating in an indoor environment. The validity of the slow coupling assumption may be questionable in this case, but its effect of the channel capacity illustrates the general trend in real channels.

We begin the analysis by studying the solutions of equation (7). The general solution is a matrix $A(z)$, where each column $\underline{A}^i(z)$ is of the form:

$$\underline{A}^i(z) = \sum_{n=1}^{L} C_n^i \underline{B}_n e^{\alpha_n z} \quad i = 1, 2 \ldots N_t \qquad (8)$$

$\underline{B}_n$ are the eigenvectors of Γ and α_n are the corresponding eigenvalues; C_n^i are scalar constants.

At large distances from the source, the modal coefficients converge to

$$\underline{A}^i(z) \to C^i \underline{B}_1 e^{\alpha_1 z} \qquad (9)$$

where α_1 is the eigenvalue of Γ that has the biggest real part. Expression (9) is the steady state solution of the coupled modes equation (7). In this solution, the only variation along the hallway is $e^{\alpha_1 z}$ (except for changes of the phase along z, which are included in Z). The steady state modal distribution has most of the power in the low order modes, because they have the least loss. We stress that (9) represents the average behavior at large distances from the transmitter. The actual behavior fluctuates around this average, where the extent of the fluctuations depends on the wall perturbations.

After convergence to steady state, the matrix A is of the form

$$A = \underline{B}_1 \left[C^1 \; C^2 \; \ldots \; C^N \right] e^{\alpha_1 z} \qquad (10)$$

and its rank equals 1. From equation (6) this implies that the channel transfer matrix T also has rank 1. At small transmitter—receiver distances the channel capacity is limited by the number of transmitter or receiver antennas [3], but at larger distances it is limited by the physics of the propagation channel. The reduced capacity results from high correlation between antennas or from a keyhole effect, depending on the environment of the transmitter and receiver, and the amount of local scattering. A similar behavior is predicted in [4], [1], where modal loss is the mechanism limiting the capacity of the channel. Another case of a bound on capacity for distant transmitter and receiver is shown in [7], where the propagation model is based on rays.

The convergence of $\underline{A}(z)$ from an initial condition to the steady state behavior is accompanied by a convergence of the power loss rate. The initial power loss rate varies along z, as the amplitudes of the different modes change. When the steady state is reached, the power loss rate sets to $2\,\text{real}(\alpha_1)$ Np/m. The convergence of the power loss rate in measurements is

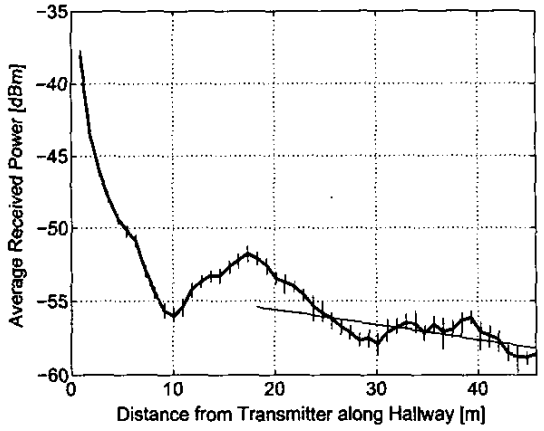

Fig. 1. Average power along the hallway. The straight line indicates the approximate steady state power loss rate. The short vertical lines indicate the minimum and maximum power levels received at each location.

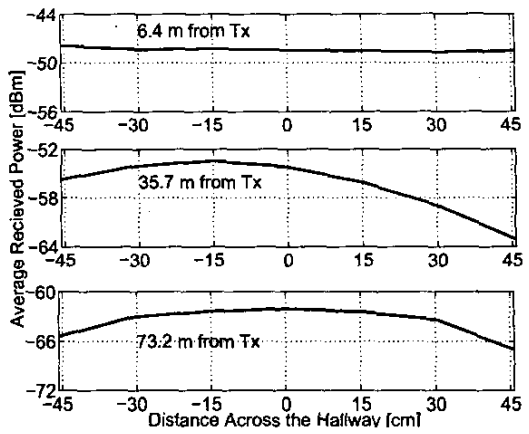

Fig. 2. Power measured across the hallway. For the top plot, the receiver is 6.4 m from the transmitter, the middle plot is at 35.7 m and the bottom plot is at 73.2 m

shown in the next section, with the reduction of capacity along a hallway.

III. Measurements

This section presents channel capacities estimated from channel measurements that were taken with a system with 12 transmit antennas and 15 receive antennas. The transmitter was located in a hallway and the receiver was located at different positions along the same hallway and in adjacent rooms, see section IV for details of the measurement equipment and locations.

Figure 1 shows the average power measured at different positions along the hallway, averaged over 100 separate measurements at each location. These results, together with others from similar office buildings, show that the power loss rate in hallways sets around 10 m from the transmitter. The variation of power in figure 1 between 10 m and 20 m corresponds to the location of a junction of hallways.

The setting of the power loss rate indicates the distance of convergence of A to the steady state. Waveforms across the hallway converge to a half sinusoidal shape as seen in figure 2. This is a consequence of the steady state modal distribution, that has most of the power in the lowest order mode.

The capacity results shown below were calculated using (2) at different locations, with the signal to noise ratio fixed at $\rho = 20$ dB. Figures 3 and 4 show the average capacity, over 100 separate measurements of the channel matrix at each location. A fixed value was used for the signal to noise ratio in order to isolate the effects of the channel from the effects of the power roll-off with distance.

Figure 3 shows the capacity calculated from the channel measurements at different locations along the hallway. The figure also contains the mean and maximum capacities calculated for a Gaussian channel with 12 transmit antennas and 15 receive antennas. The maximum capacity is calculated for a full rank

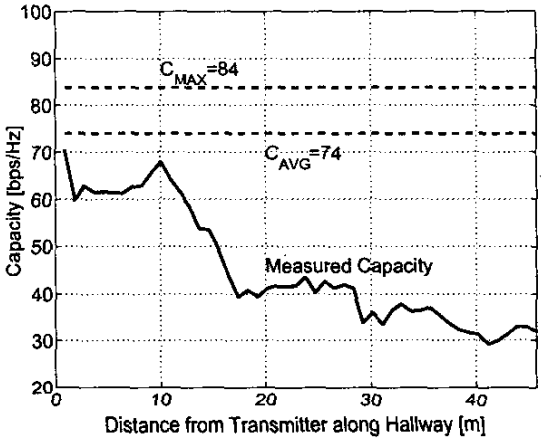

Fig. 3. Average capacity of the measured channel in the hallway for SNR=20 dB, receiver array facing east.

channel with equal eigenvalues and the mean capacity is taken over all channels with independent Gaussian entries in the channel matrix. The graph shows a reduction in capacity along the hallway.

Figure 4 shows capacity results for the channel measured in the laboratory rooms adjacent to the hallway (see the schematic plan in figure 6). The horizontal axis contains the transmitter – receiver separations along the hallway. Four different graphs are shown, for the four orientations of the receiver array. The results for the four orientations are similar.

The capacity in the rooms adjacent to the hallway drops with increasing distance from the transmitter. The effect of the power level was excluded so the reduction of capacity values seen here is the result of variations in the channel matrix.

The decrease of capacity with distance (figures 3, 4) is the result of the propagation mechanism. Most of the power in the rooms was leaked from the hallway, through the wallboards, so

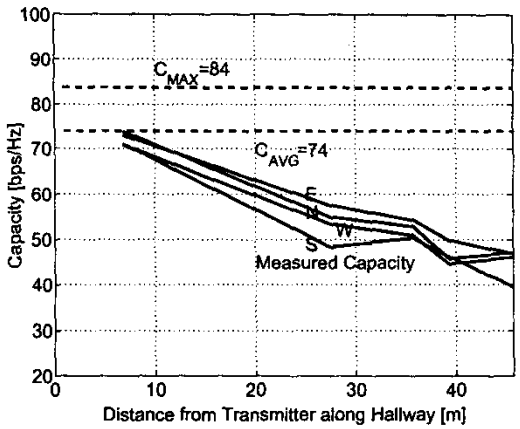

Fig. 4. Average capacity of the measured channel in the labs for SNR=20 dB, for the receiver antenna facing the four cardinal directions.

a low rank channel at a certain location in the hallway causes low capacities in nearby rooms.

The measured receiver correlation is low (<0.25) for all measurements. Transmitter correlation cannot be estimated directly from the measurements, but it is similar to the receiver correlation in the hallway because of the symmetric geometrical arrangement of the two arrays.

IV. The Measurement Setup and Environment

Many details were omitted form the descriptions below, because of space considerations. For a full description of the measurements see [8].

1) Description of the Measuring Equipment: The measurements were taken with two antenna arrays: the transmitter array comprised 12 elements arranged on the sides of a square, and the receiver array comprised 15 elements arranged in a grid. Adjacent antennas were separated by 8 cm, and the elements on both arrays were arranged with alternate polarizations. Figure 5 shows the transmitter and the receiver arrays as seen from the front where V and H stand for vertically and horizontally polarized elements. The two arrays were placed at a height of 2m. The system bandwidth was 30 kHz, the filters were raised cosine filters with a bandwidth expansion factor of $\alpha = 0.23$; the symbol rate was 24.3 ksymbols/sec, which is low enough to support the narrowband assumption. The constellation size used was 4 QPSK and the operating frequency was 1.95 GHz.

2) Description of the Measuring Process: The measurements were taken within the Lucent Crawford Hill Building. The hallway measurements were taken in the building's second floor main corridor, shown schematically in figure 6. This straight 119 m corridor is 1.8 m wide, lined with offices (typically 3 m×3 m) on one side and laboratories (typically 3.5 m×7.5 m) on the other. A second corridor intersects the first one in a T shaped junction, but no measurements were taken in that environment. The building extends in both the east and the

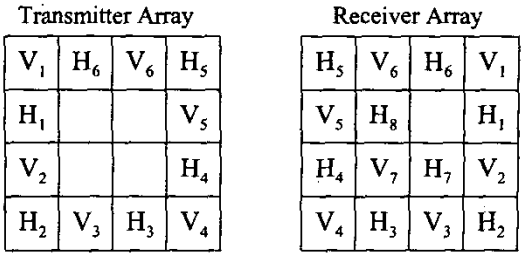

Fig. 5. Antenna array layout, V and H represent different polarizations.

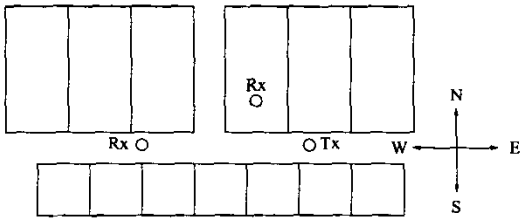

Fig. 6. Geometry of hallways with the transmitter location and two receiver locations

west direction, and the second corridor extends in the north direction and is also lined with labs and offices. Inside walls were made of wallboard, outside walls were mainly glass. Ceilings and floors were reinforced concrete, with solid corrugated steel pour forms permanently in place between floors and in the roof.

The transmitter was placed 21.4 m from the eastern end of the hallway and 60 cm from the northern wall of the hallway, pointing west. The transmitter was kept at this location for all the hallway and lab measurements. For the lab measurements, the receiver was wheeled to the desired lab and was positioned 2.4 m north of the east-west line defined by the transmitter.

The data was transmitted in bursts of 100 symbols. In order to calculate the channel complex gains, the first 20 symbols of each burst were devoted to training. Since the transmitted signals are fully co-channel (all antennas transmit simultaneously within the same frequency band), the channel estimation was performed using orthogonal training sequences as suggested in [9]. After the receiver had learnt the channel with the training process, the payload data (the last 80 symbols of each burst) were decoded using the V-BLAST algorithm, but we are interested here only in the channel properties as indicated in the measured channel transfer matrix.

The signal power was set to a sufficient value to guarantee a signal to noise ratio of at least 15 dB. This was done in order to guarantee the accuracy of our capacity calculation [10]. For each measurement location, about 100 bursts (100 instantiations of the channel transfer matrix T) were recorded in order to average over the small scale temporal variation (doors opening and closing, people walking through the hallway or in the labs etc).

In order ot estimate the receiver antenna correlation, the measurements were repeated with the receiver moved over a grid

of 21 locations (in the hallway) or 33 locations (in the labs), with the points 15 cm from each other. The transmitter was not moved similarly, so transmitter correlations cannot be calculated.

V. Conclusions

The coupling among propagating modes in a waveguide reduces the channel capacity along the waveguide. A multiple antenna system operating in a building hallway shows diminishing capacities as the distance between the transmitter and the receiver grows. This decrease in capacity is the result of a keyhole effect caused by mode coupling, and the decrease of power levels at growing distances from the transmitter. The keyhole effect is explained using a propagation model based on the waveguide properties of the hallway.

Measurements of power levels along indoor hallways indicate that the power distribution among the modes sets to its steady state at distances in the order of 10 m from the transmitter and the effective rank of the channel is expected to set to its steady state value around the same area.

The capacity was estimated from channel measurements, and a decrease is apparent along the hallway with growing distances from the transmitter. This decrease occurs in the hallway as well as in the rooms located beside it. We suggest that the main propagation mechanism into the rooms is leakage from the hallway, through the interior walls of the building. A keyhole effect in the hallway limits the capacities measured along it and in the rooms.

References

[1] D. Chizhik, G. J. Foschini, M. J. Gans, and R. A. Valenzuela, "Keyholes, correlations and capacities of multi-element transmit and receive antennas," in *Vehicular Technoloty Conference*, 2001 Spring, vol. 1, pp. 284–287.

[2] D. Gesbert, H. Bölcskei, and A. Paulraj, "MIMO wireless channels: Capacity and performance prediction," in *Global Telecommunications Conference*. IEEE, 2000, vol. 2, pp. 1083–1088.

[3] G. J. Foschini and M. J. Gans, "On limits of wireless communications in a fading environment when using multiple antennas," *Wireless Personal Communications*, vol. 6, no. 3, pp. 311–335, March 1998.

[4] P. Kyritsi and D. C. Cox, "Modal analysis of MIMO capacity in a hallway," in *Global Telecommunications Conference*. IEEE, 2001, vol. 1, pp. 567–571.

[5] D. Porrat and D. C. Cox, "A waveguide model for UHF propagation in streets," in *The 11th Virginia Tech/MPRG Symposium on Wireless Personal Communications*, June 6-8 2001, Blacksburg, Virginia.

[6] D. Marcuse, "Mode conversion caused by surface imperfactions of a dielectric slab waveguide," *The Bell System Technical Journal*, pp. 3187–3215, December 1969.

[7] Da-Shan Shiu, Gerard J. Foschini, Michael J. Gans, and Joseph M. Kahn, "Fading correlation and its effect of the capacity of multielement antenna systems," *IEEE Transactions on Communications*, vol. 48, no. 3, pp. 502–512, March 2000.

[8] P. Kyritsi, *Multiple Element Antenna Systems in an Indoor Environment*, Ph.D. thesis, Stanford University, 2001.

[9] T.L. Marzetta, "Blast training: Estimating channel characteristics for high capacity space-time wireless," in *37th Annual Allerton Conference on Communication, Control and Computing*, Monticello, IL, September 1999, IEEE.

[10] P. Kyritsi, R.A. Valenzuela, and D.C. Cox, "Effect of channel estimation on the accuracy of capacity estimation," in *Vehicular Technology Conference*, Kluwer Academic Publishers, Ed., Rhodes, Greece, May 2001, IEEE.